Appl. Phys. B (2016) 122:256
DOI 10.1007/s00340-016-6529-2

Applied Physics B
Lasers and Optics

Investigation of the femtosecond optical limiting properties of monoclinic copper niobate

N. Priyadarshani[1] · S. Venugopal Rao[2] · T. C. Sabari Girisun[1]

Received: 22 March 2016 / Accepted: 14 September 2016

Abstract Investigation of the third-order nonlinear optical properties and optical limiting behaviour of microstructured monoclinic phase copper niobate ($CuNb_2O_6$) was performed by the Z-scan technique using femtosecond laser pulses (800 nm, 150 fs, 80 MHz). $CuNb_2O_6$ was synthesized by solid-state reaction at a sintering temperature of 700 °C maintained at different times of 3, 6, 9 and 12 h. Formation of rods at higher reaction time of 12 h was observed and is attributed to the mass transport and coalescence processes. From the absorption tail of UV–Vis spectrum, the optical band gap was estimated to be 3.5 eV. In the fluorescence spectra, blue emission was observed near 430 nm and was assigned to the charge transfer from oxygen to central niobium of Nb-O_6 octahedra. Open-aperture Z-scan data demonstrated the presence of nonlinear absorption in copper niobate and are ascribed to two-photon absorption process. Closed-aperture data indicated a sign reversal in nonlinear refraction as the sintering time increased. Third-order nonlinear optical coefficients were estimated, and the largest coefficient was observed for the rod-structured $CuNb_2O_6$. Copper niobate exhibited optical limiting behaviour, and the limiting threshold was found to be lowest for microrod structures (~0.21 μJ/cm^2). Due to the top-notch third-order nonlinear optical coefficients and excellent limiting behaviour, monoclinic copper niobate microrods can be used as a potential material for utilization as an optical limiter for femtosecond pulses.

Electronic supplementary material The online version of this article (doi:10.1007/s00340-016-6529-2) contains supplementary material, which is available to authorized users.

✉ T. C. Sabari Girisun
sabarigirisun@bdu.ac.in

S. Venugopal Rao
soma_venu@uohyd.ac.in

[1] Nanophotonics Laboratory, School of Physics, Bharathidasan University, Tiruchirappalli 620021, India

[2] Advanced Centre of Research in High Energy Materials (ACRHEM), University of Hyderabad, Hyderabad, Telangana 500046, India

1 Introduction

Utilization of lasers has increased many folds in the fields of medicine, industry, aviation, communications and defence sectors. Among the various available lasers, ultrashort pulsed lasers with the pulse durations of few femtoseconds (fs) to few hundred fs are in high demand in industries and research laboratories. Applications of these lasers are vast in a variety of areas such as material processing, laser direct writing, selective laser etching, glass welding, sub-surface marking and surface texturing [1, 2]. In particular, these lasers find extensive usage in the field of medicine for cancer detection, cell transfection, collagen imaging, microsurgery, tissue welding, cataract surgery and refractive vision correction [3, 4]. Although these lasers are never directly interacting with humans, the risk of accidents is very high since these lasers release an enormous amount of energy at short duration. Therefore, the scientific community has been investigating various methodologies including efficient passive-optical limiting materials, which block the transmittance of high-intensity light and allow the low-intensity light to pass through. Organic materials such as phthalocyanines [5], fullerenes [6] and carbon nanotubes [7] are some of the well-known optical limiters as these have demonstrated low limiting thresholds and strong nonlinear optical (NLO) coefficients. The major concern of organic materials-based optical limiters is its

Published online: 26 September 2016

small dynamic range as it has low laser damage threshold. Hence, as an alternate, inorganic materials are under recent focus due to their high thermal and mechanical stability.

Among the inorganic systems, niobate materials such as lithium niobate, potassium niobate and sodium niobate are the well-known NLO materials as it has wide spectral coverage and large electro-optic coefficients [8, 9]. Especially, niobates of AB_2O_6 (A-metal, B-niobates) form having perovskite structure are under recent attraction because of its spontaneous polarization and high optical nonlinearities. In the choice of metals for niobate, copper is advantageous in optical limiters as it can provide broad spectral range, high thermal stability and strong anti-photo corrosive nature [10]. Also literature reveals that the addition of copper enhances the nonlinear absorption and the first report on the optical limiting behaviour of CuO thin films in the femtosecond (fs) regime demonstrated a low limiting threshold of 0.3 GW/cm^2 [11]. Similarly, nonlinear absorption of copper phthalocyanine was investigated in the fs regime both experimentally and theoretically which showed large fifth-order NLO coefficient [12]. Based on these facts, it can be proposed that copper niobate can be used as broad band limiters as it has broad spectral range, high thermal stability and excellent anti-photo corrosive nature. Another advantage of this material is that its optical properties can be tuned by varying its microstructure, and in particular, one-dimensional structure will have enhanced nonlinear optical behaviour as the incident field is fully coupled to the local mode. Although copper niobate has been intensively studied for their applications in solar cell and gas sensing, the NLO properties of this material and the origin of the optical nonlinearity have not been studied till date. This article reports the preparation of one-dimensional microstructures of monoclinic phase copper niobate by varying the sintering time of solid-state reaction. Also their third-order optical nonlinearity and optical limiting behaviour in the femtosecond regime were studied by Z-scan technique.

2 Preparation and methods

For the preparation of pure monoclinic phase of copper niobate, copper oxide and niobium metal of analytical grade were taken as starting material. The finely grinded precursor was kept in a furnace at 700 °C for various sintering time (3, 6, 9 and 12 h). The obtained powders appeared to be yellowish green in colour [13]. The preliminary identification and phase confirmation of the compound were carried out by PAN Analytical X-Ray powder diffractometer. The prepared samples were subjected to FESEM with EDS analysis for morphological and elemental studies by FEI Quanta FEG 200 scanning electron microscope. The absorption and emission spectra of the 1 mg copper niobate dispersed in 1 µl of diethylene glycol were studied using LAMDA UV–Vis–NIR spectrophotometer and JASCO spectrofluorometer, respectively. Nonlinear optical (NLO) studies were performed by the standard Z-scan experiment using ultrashort pulses delivered by a Ti:sapphire (800 nm, 80 MHz, 150 fs, 3–4 mW) laser source, and the pulses were focused using a plano-convex lens of focal length 10 cm with beam waist $\left(\omega_0 = \frac{f\lambda}{\pi d}\right)$ of ~26 µm. All the four samples of 1 mg weight were dispersed in 1 ml of diethylene glycol such that their linear transmission was ≥70 %. The sample was taken in 1-mm quartz cuvette for performing open- and closed-aperture Z-scan experiments. The sample was slowly moved along the Z-axis (between +Z and −Z) of the laser beam using the linear translation stage. The change in light transmission for every corresponding Z-position was monitored using pyroelectric energy detector, and the experiments were repeated several times to assure the reproducibility of results. Depending on the Z-position, intensity of the laser falling on the material varies with the intensity being maximum at the beam focus. For all the samples, similar peak intensities were maintained and the detailed experimental procedure is reported elsewhere [14].

3 Structural and morphological studies

The recorded EDS spectrum (provided in the supplementary data) confirmed the presence of copper, niobium and oxygen in the prepared materials. The preliminary identification and phase confirmation of the materials were made with the XRD analysis (provided in the supplementary data). All the peaks in the pattern were identified and indexed using the JCPDS card no: 83-0369 [15]. The formation of pure monoclinic phase copper niobate without any traces of Nb_2O_5, CuO, Nb and orthorhombic $CuNb_2O_6$ was configured. Figure 1 presents the FESEM images of the samples prepared at various sintering times. It can be clearly seen that at higher sintering time of 12 h (Fig. 1a), microrod-like structures were observed because of densification and coalescence processes. To further understand the growth mechanism, FESEM image of the samples obtained at other sintering times of 3–9 h was analysed. At 3-h sintering time (Fig. 1b), local bonding formed between the particles creating pore-like structure due to mass transport and densification process [16]. At 6-h sintering time (Fig. 1c), densification further increased, resulting in the minimization of pore diameter along with the formation of nucleation sites. Well-defined pores along with the formation of rod were identified for the 9-h sintered material (Fig. 1d) due to coalescence process. Thus, as sintering time increased, densification and coalescence processes occurred simultaneously, resulting in the formation of well-grown microrod structures.

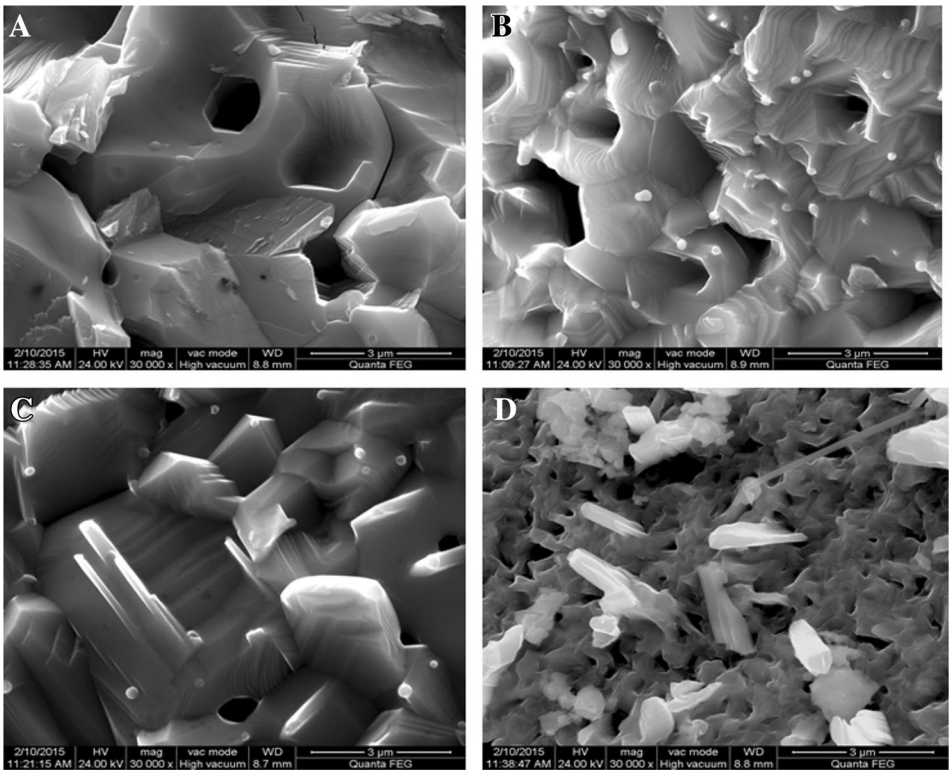

Fig. 1 FESEM image (with *scale bar* of 3 μm) of copper niobate obtained at **a** 3 h, **b** 6 h, **c** 9 h and **d** 12 h

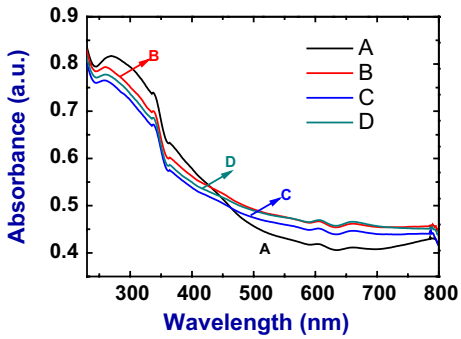

Fig. 2 UV–Vis absorption spectrum of copper niobate sintered at **a** 3 h, **b** 6 h, **c** 9 h and **d** 12 h

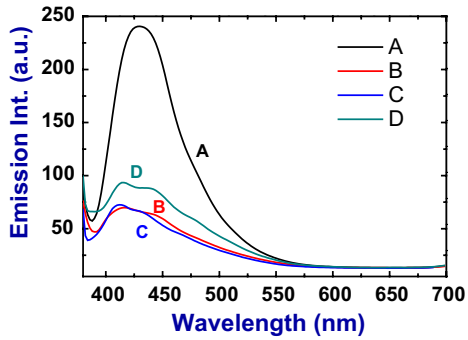

Fig. 3 Emission spectra of copper niobate sintered at **a** 3 h, **b** 6 h, **c** 9 h and **d** 12 h

4 Linear optical properties

The recorded UV–Vis–NIR absorption spectra of the prepared materials are shown in Fig. 2. A broad UV absorption around 250–400 nm was due to charge transfer from the oxygen ligand of the octahedron corner to the central niobium atom [17]. From the absorption edge, the optical band gap of copper niobate was estimated to be 3.55 eV. Change in the morphology does not alter the position of the absorption edge to great extent and hence no sharp variation was observed in the optical band gap of the materials. Figure 3 represents the emission spectra of the samples. A strong emission band at $\lambda_{em} = 430$ nm (2.8 eV) for the excitation wavelength of $\lambda_{ex} = 360$ nm was observed. Similar pattern was reported for $ZnNb_2O_6$ [18] and $NiNb_2O_6$ [19] in which the emission band was observed around 445 and 440 nm, respectively. In general, AB_2O_6 materials consist of two octahedral chains with AO_6 and BO_6 moieties, in which BO_6 is responsible for its luminescence property. In our case, CuO_6 and NbO_6 link each other forming a long chain along the (100) direction sharing the edges and corners. Hence, the possible luminescence property was due to edge-shared NbO_6 octahedra which accredits due to self-trapped exciton recombination because of high relaxation in the excited state.

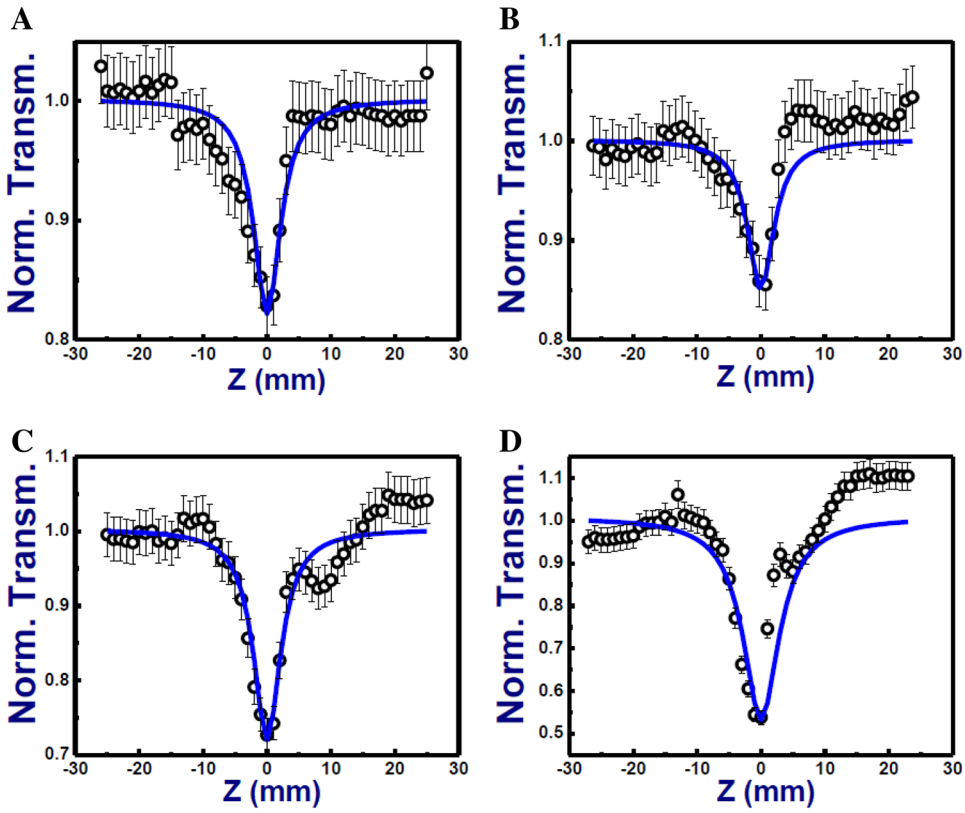

Fig. 4 Open-aperture Z-scan pattern of copper niobate obtained at **a** 3 h, **b** 6 h, **c** 9 h and **d** 12 h

5 Third-order NLO properties and optical limiting studies

The third-order NLO properties of monoclinic phase copper niobate ($CuNb_2O_6$) were investigated by using the standard Z-scan technique. The closed and open aperture data were recorded with and without aperture respectively and graphs were drawn between position and normalized transmission. In the open-aperture Z-scan data presented in Fig. 4, transmission of the samples gradually decreased towards the focal point and formed a strong valley pattern was observed for all the prepared samples. The valley pattern showed a significant change and gets deeper with an increase in sintering time. Since the Z-scan experiments were carried out using a pulse width of ~150 fs, the observed nonlinearity is expected to have predominant contribution from the electronic transitions in these materials along with some thermal contribution due to the high repetition rate. With ultrafast laser pulse excitation, nonlinear absorption in the samples may arise due to various nonlinear optical mechanisms like two-photon absorption, three-photon absorption, excited state population. In Fig. 4, the open circles indicate the recorded experimental data points and the starred lines represent the theoretical fits drawn based on Sheik-Bahae formalism [20]. The two main advantages of Sheik-Bahae formalism (SBF) was that it directly monitors the radiation intensity within the medium and it avoids the need of slowly varying envelope approximation (SVEA) approximation. The normalized transmittance for multi-photon absorption was calculated using the relation [20].

$$T_{nPA} = \frac{1}{\left[1 + (n-1)a_n L \left(\frac{I_o}{1+\left(\frac{z}{z_0}\right)^2}\right)^{n-1}\right]^{\frac{1}{n-1}}}$$

where α_n is the nonlinear absorption coefficient with $n = 2, 3$ for two-photon absorption (2PA) and three-photon absorption (3PA), respectively, L is the thickness of the sample, $Z_0 = \pi\ \omega_0^2/\lambda$ is Rayleigh length and I_0 is the incident intensity of the laser beam at focus.

In the present case, the theoretical fit for the experimental data was found to be best fit for two-photon absorption (2PA) equation. The excitation photons energy (800 nm, 1.55 eV) is less than the half of the band gap of the material (3.5 eV). In the emission spectrum (data shown in Fig. 3), the absorption peak in the vicinity of 430 nm (2.8 ± 0.5 eV due to its broad band) recorded could be attributed to the self-trapped excitons due to transfer of charge from oxygen ligands to the niobium at the centre. Therefore, under 800 nm (1.55 ± 0.3 eV, due to certain bandwidth associated with the fs pulses) excitation, the optically pumped electrons get excited from the ground state and transit to intermediate states (self-trapped exciton states) by absorbing

Table 1 Third-order NLO coefficients of copper niobate ($CuNb_2O_6$) microstructures

Sintering time	$\beta_{eff} \times 10^{-10}$ m/W	$n_2 \times 10^{-12}$ m^2/W	Re [$\chi^{(3)}$] $\times 10^{-18}$ m^2/V^2	Im [$\chi^{(3)}$] $\times 10^{-18}$ m^2/V^2	$\chi^{(3)} \times 10^{-10}$ esu	Limiting threshold (μJ/cm^2)
3 h Sample A	20.00 ± 0.60	−6.11 ± 0.18	−8.42 ± 0.25	1.75 ± 0.05	6.16 ± 0.18	0.76 ± 0.01
6 h Sample B	20.50 ± 0.62	−2.35 ± 0.07	−3.25 ± 0.98	1.80 ± 0.05	2.67 ± 0.08	0.54 ± 0.01
9 h Sample C	33.00 ± 0.99	3.46 ± 0.10	4.78 ± 0.14	2.90 ± 0.09	4.00 ± 0.12	0.31 ± 0.01
12 h Sample D	85.00 ± 2.55	4.13 ± 0.12	5.70 ± 0.17	7.48 ± 0.22	6.74 ± 0.20	0.21 ± 0.01

two simultaneous photons. Another possibility is the presence of surface/defect states near the band gap which satisfies the energy condition required for 2PA process to occur. Z-scan experiment by itself cannot distinguish genuine and sequential 2PA (wherein two photons are absorbed with small time delay with the population staying in the excited state for a finite period of time [21–23]). The possibility of two-step two-photon absorption with 150-fs pulses is negligible since the pulse duration is too short and the lifetime of population in the excited state (virtual states in this case) is shorter (typically <100 fs) than the pulse duration. The excess energy available during the transition could be emitted as non-radiative energy (preferably thermal dissipation). Here the additional energy redistributes, among the various vibrations in the solute molecules and turns into intramolecular heat. The intramolecular heat eventually dissipates into the phonon bath and raises the solution temperature since molecular vibrations are ultimately coupled to thermal phonons in the solution [24]. The estimated two-photon absorption coefficient (β_{eff}) values from the theoretical fits are presented in Table 1. It can be seen that the β_{eff} value constantly increased with increase in sintering time. For the microstructures with rod formation, a drastic increase in the nonlinear absorption coefficient was observed. A similar type of enhanced nonlinear absorption coefficient (5.9×10^{-7} cm/W) was witnessed for ZnO nanorods which showed 100 times higher coefficient than its nanoparticles with fs laser pulse excitation [25].

To figure out the sign and magnitude of nonlinear refractive index (n_2), closed-aperture Z-scan experiment was performed by keeping the aperture in front of the detector. Figure 5 shows the closed-aperture Z-scan profile of the sintered materials. In the closed-aperture pattern, pre-focal maxima (peak) followed by post-focal minima (valley) suggests that the material possesses negative nonlinearity with self-defocusing behaviour and the valley-peak pattern will have positive nonlinearity with self-focusing behaviour [26]. These self-actions are because of the nonlinear polarization induced by the incident beam. It is interesting to note that the sign reversal in nonlinear refraction took place as the sintering time increases. Materials obtained at sintering time of 3 and 6 h having pore-like structure endow with negative nonlinearity, while the sintered samples obtained at 9 and 12 h with the rod structure show positive nonlinearity. The obtained result suggests that the rod structure obtained due to densification and coalescence favours self-focusing behaviour. Based on the equations suggested in Sheik-Bahae formalism [27], the normalized transmittance was theoretically estimated using the relation,

$$T_{CA} = 1 \pm \frac{4\Delta\phi\left(\frac{z}{z_0}\right)}{\left[1+\left(\frac{z}{z_0}\right)^2\right]\left[9+\left(\frac{z}{z_0}\right)^2\right]}$$

where z is the distance moved from the focus ($z = 0$) by the sample, z_0 is the Rayleigh range and $\Delta\Phi$ is the phase change of the laser beam due to refraction. Usually, the closed-aperture Z-scans were performed with low peak intensities to avoid any nonlinear absorption contribution. Further, the closed-aperture data were divided by open-aperture data (recorded with similar peak intensities) in case if there is any contribution involved, even though minor were felt. Also in all the cases, the value of $\Delta\Phi$ was ensured to be less than π. In Fig. 5, the solid lines represent the theoretical fits obtained using the above-mentioned equation and open circles denote the experimental data. Usually, the sign reversal is associated with the values of nonlinear refractive index (n_2) which have a dependence on the temperature of the material. In this experiment, thermo-optic effect cannot be completely neglected because high repetition rate of 80 MHz was used in excitation source. It is fascinating to note that the sign of nonlinear refractive index switches from negative to positive, and hence, the sintering time not only plays a key role in formation of rods, but also in the signature of nonlinear refractive index of the material. The estimated nonlinear refractive index values were found to be in the range of 10^{-13}–10^{-12} m/W, and the data are summarized in Table 1. One of the possible reasons for the observed shift from negative to positive nonlinearity depending on the formation of rod structure

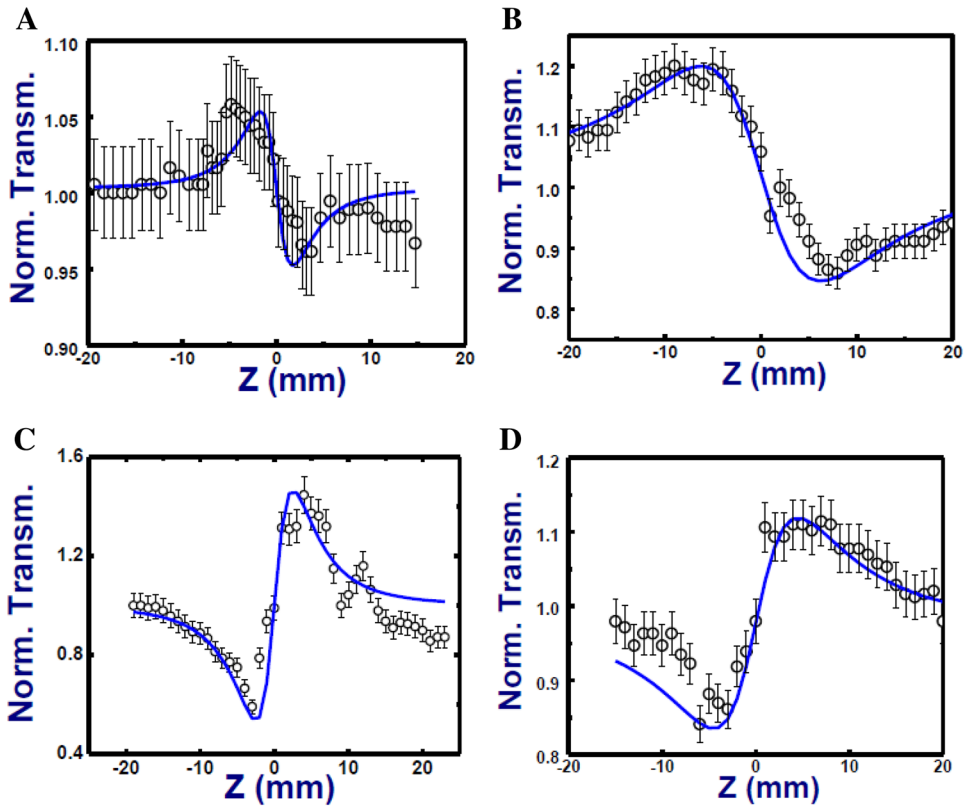

Fig. 5 Closed-aperture Z-scan pattern of copper niobate obtained at **a** 3 h, **b** 6 h, **c** 9 h and **d** 12 h

could be due to the change in the inter-atomic distances. As the sintering time was increased (9 and 12 h), due to further densification followed by coalescence process, the micropore structures transformed themselves into microrod structures. Therefore, the distance between the inter-atomic planes changed thereby producing a variation in the binding potential. This in turn possibly switched the refraction mechanism and produces a variation in the value of nonlinear refractive index (n_2) due to minute displacement of the electronic cloud. Furthermore, in one-dimensional rod-like structure, the thermal nonlinearity is large because of quick thermal dissipation arising from incident beam being fully coupled to local mode. Hence, the sample with rod formation suffered sign reversal as well as enhancement of optical nonlinearity compared to other microstructures [28].

Third-order NLO susceptibilities ($\chi^{(3)}$) of the sintered materials were calculated from nonlinear refractive index and nonlinear absorption coefficient using the standard relations [29]. The estimated third-order NLO coefficients are presented in Table 1. The error bars are indicative of the small uncertainties in the experimental values resulting from (a) beam waist estimation, (b) fitting procedures, (c) input energy fluctuations, etc. It is worthy to note that, compared to other microstructures of copper niobate, rods showed enhanced third-order NLO susceptibility as the incident field is fully coupled to the local mode in one-dimensional structure. Also the real part of nonlinear optical susceptibility was found to be higher than its imaginary part, suggesting the dominance of nonlinear refraction than nonlinear absorption in the material. Such scenarios are usually expected at higher repetition rate (80 MHz) of laser excitations. A similar observation of enhanced third-order optical nonlinearity in nano-/micro-ZnO rods due to large polarization effect in fs regime (800 nm, 50 fs, 1 kHz) was reported recently [30]. The third-order NLO susceptibility values of copper niobate samples obtained with fs excitation were compared with other semiconductor materials like CdS (9.8×10^{-14} esu) [31], CS_2 (9.8×10^{-14} esu) [32], CuO (10^{-18} esu) and Cu_2O (10^{-19} esu) [33] where the susceptibility of monoclinic copper niobate depicted higher third-order nonlinearity. This is because materials such as Nb_2O_5/Ta_2O_5 and V_2O_5 depict higher NLO coefficients due to the metal–oxygen bond length where the atoms of metal and oxygen atoms are co-ordinated octahedrally [34].

Optical limiting is a nonlinear behaviour of a material through which it allows low-intensity light to pass through while blocking high-intensity light, and the point of deviation is defined as the limiting threshold of the material. Figure 6 portrays the optical limiting curve drawn between normalized transmittance and the input laser fluence extracted from the recorded open-aperture data using the standard equations [35]. Initially, for the low input irradiance, output energy was linearly

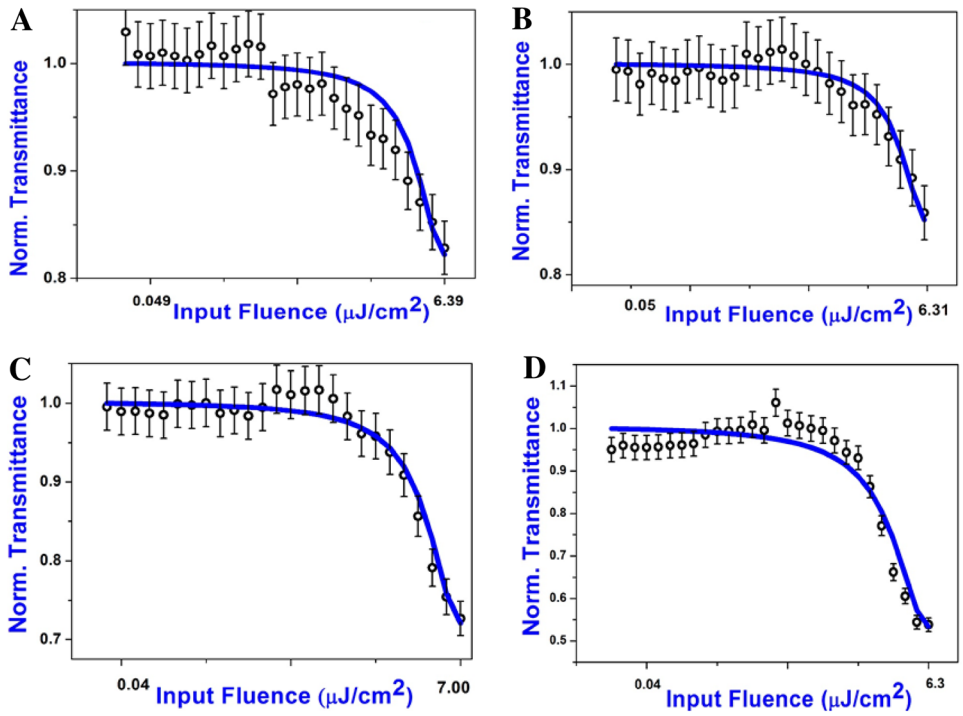

Fig. 6 Optical limiting pattern of copper niobate obtained at **a** 12 h, **b** 3 h, **c** 6 h and **d** 9 h. *Dotted lines* are the experimental data, and *solid lines* indicate the numerical fits

proportional to input and beyond certain point, and the curve deviates from its linear behaviour confirming the optical limiting behaviour of the material. All the four prepared copper niobate samples show a strong limiting behaviour with a sound variation in the limiting threshold (0.21–0.76 μJ/cm^2). Also optical limiting threshold of copper niobate was found to much lower than limiting materials such as bismuth nanospheres (2.16 μJ/cm^2) [36], zinc oxide thin film (128 μJ/cm^2) [37] and Duran glass (35 μJ/cm^2) [38] irradiated under similar condition. Hence, it can be clearly witnessed that one-dimensional rod structure copper niobate showed enhanced nonlinear optical behaviour with low limiting threshold and it can be a good alternate for benchmark limiter like CNT suspension [39].

6 Conclusions

In summary, the third-order NLO properties and optical limiting behaviour of copper niobate with various microstructure were studied by Z-scan technique using Ti:sapphire laser pulses (800 nm, 150 fs). Earlier, FESEM analysis illustrated the formation of microrods at higher sintering time due to the occurrence of densification and coalescence process. The threshold of the limiting properties of microrod copper niobate was found to be lowest than other microstructures and well-known limiters. The observed limiting behaviour of copper niobate was due to the contribution of 2PA absorption. Increase in depth of the valley pattern depicted the enhancement of nonlinear absorption with drastic variation in the nonlinear absorption coefficient (20–85 $\times$ 10^{-10} m/W). Interestingly, formation of rods switched the nonlinear refraction from self-defocusing to self-focusing behaviour. Also the third-order NLO susceptibility (1.36 $\times$ 10^{-10} esu) was estimated to be higher for microrod structure since the incident light is fully coupled in 1D structure. The present study demonstrates that a significant change in the NLO coefficients and limiting threshold of copper niobate can be achieved by tuning the microstructures. In particular, one-dimensional microrod copper niobate with enhanced nonlinear behaviour can be used as a potential optical limiter in the fs regime.

References

1. C. Hnatovsky, R.S. Taylor, E. Simova, P.P. Rajeev, D.M. Rayner, V.R. Bharadwaj, P.B. Corkum, Fabrication of microchannels in glass using forced femtosecond laser radiation and selective chemical etching. Appl. Phys. A **84**, 47–61 (2006)
2. K.M. Davis, K. Miura, N. Sugimoto, K. Hirao, Writing waveguides in glass with a femtosecond laser. Opt. Lett. **21**, 1729–1731 (1996)
3. I.V. Ilina, A.V. Ovchinnikov, D.S. Sitnikov, M.M. Rakityanskiy, M.B. Agranat, Y.V. Khramova, M.L. Semenova, Application of femtosecond laser pulses in biomedical cell technologies. High Temp. **51**, 173–178 (1996)
4. T.V. Roberts, M. Lawless, S.J. Bali, C. Hodge, G. Sutton, Surgical outcomes and safety of femtosecond laser cataract surgery: a prospective study of 1500 consecutive cases. Opthamology **120**, 227–233 (2013)

5. N. Venkatram, D. Narayana Rao, L. Giribabu, S. Venugopal Rao, Femtosecond nonlinear optical properties of alkoxy pthalocyanines at 800 nm studied using Z-Scan technique. Chem. Phys. Lett. **464**, 211–215 (2008)
6. E. Koudoumas, M. Konstantaki, A. Mavromanolakis, X. Michaut, S. Couris, S. Leach, Transient and instantaneous third-order nonlinear optical response of C_{60} and the higher fullerenes C_{70}, C_{76} and C_{84}. J. Phys. B At. Mol. Opt. Phys. **34**, 4983–4996 (2001)
7. K.C. Chin, A. Gohel, W.Z. Chen, H.I. Elim, W. Ji, G.L. Chong, C.H. Sow, A.T.S. Wee, Gold and silver coated carbon nanotubes: an improved broad-band optical limiter. Chem. Phys. Lett. **409**, 85–88 (2005)
8. G.S. Maciel, N. Rakov, C.B. de Araujoa, A.A. Lipovskii, D.K. Tagantsev, Optical limiting behavior of a glass–ceramic containing sodium niobate crystallites. Appl. Phys. Lett. **79**, 584–586 (2001)
9. M. Imlau, H. Badorreck, C. Merschjann, Optical nonlinearities of small polarons in lithium niobate. Appl. Phys. Rev. **2**, 040606 (2015)
10. U.A. Joshi, P.A. Maggard, $CuNb_3O_8$: a *p*-type semiconducting metal oxide photoelectrode. J. Phys. Chem. Lett. **3**, 1577–1581 (2012)
11. A. Chen, G. Yang, H. Long, F. Li, Y. Li, P. Lu, Nonlinear optical properties of laser deposited CuO thin films. Thin Solid Films **15**, 4277–4280 (2009)
12. F. Li, P. Lu, H. Long, G. Yang, Y. Li, Q. Zheng, Nonlinear absorption in CuPc-doped PMMA thin film in the femtosecond regime: experimental and theoretical studies. Opt. Express **16**, 14571–145781 (2008)
13. M.G.B. Drew, R.J. Hobson, V.T. Padayatchy, Synthesis, structure and magnetic properties of monoclinic $CuNb_2O_6$ and the electronic spectra of both polymorphs of $CuNb_2O_6$. J. Mater. Chem. **11**, 1779–1783 (1995)
14. D. Swain, T. Sarma, P.K. Panda, S. Venugopal Rao, Ultrafast excited state dynamics and dispersion studies of nonlinear optical properties in dinaphthoporphycenes. Appl. Phys. Lett. **100**, 141109–141113 (2012)
15. S. Biswas, P. Pramanik, Studies on the gas sensing behaviour of nanosized $CuNb_2O_6$ towards ammonia, hydrogen and liquefied petroleum gas. Sens. Actuators B Chem. **133**, 449–455 (2008)
16. G.L. Messing, A.J. Stevenson, Material science: toward pore-free ceramics. Science **322**, 383–384 (2008)
17. Y. Su, X. Xin, Y. Wang, T. Wang, X. Wang, Unprecedented catalytic performance in disordered nickel niobate through photosynergistic promotion. Chem. Commun. **50**, 4200–4202 (2014)
18. Y. Zhou, Z. Qiu, M. Lu, Q. Ma, A. Zhang, G. Zhou, H. Zhang, Z. Yang, Photoluminescence characteristics of pure and dy-doped $ZnNb_2O_6$ nanoparticles prepared by a combustion method. J. Phys. Chem. C **111**, 10190–10193 (2007)
19. Y. Zhao, M. Lu, Z. Qiu, A. Zhang, Q. Ma, H. Zhang, Z. Senyan, Photoluminescence of $NiNb_2O_6$ nanoparticles prepared by combustion method. Mater. Sci. Eng. B **140**, 128–131 (2007)
20. R. Sai Santosh Kumar, S. Venugopal Rao, L. Giribabu, D. Narayana Rao, Femtosecond and nanosecond nonlinear optical properties of alkyl phthalocyanines studied using Z-scan technique. Chem. Phys. Lett. **447**, 274–278 (2007)
21. M. Saravanan, T.C. Sabari Girisun, Nonlinear optical absorption and optical limiting properties of cadmium ferrite. Mater. Chem. Phys. **160**, 413–419 (2015)
22. D. Swain, R. Singh, V.K. Singh, N.V. Krishna, L. Giribabu, S. Venugopal Rao, Sterically demanded zinc(II)phthalocyanines: synthesis, optical, electrochemical, nonlinear optical, excite state dynamics studies. J. Mater. Chem. C **2**, 1711–1722 (2014)
23. S. Hamad, G. Krishna Podagatlapalli, Surya P. Tewari, S. Venugopal Rao, Influence of picosecond multiple/single ablation on Copper nanoparticles and nanostructures fabricated for surface enhanced Raman spectroscopy and photonics applications. J. Phys. D Appl. Phys. **46**, 485501 (2013)
24. M. Shui, X. Jin, Z. Li, J. Yang, G. Shi, X. Zhang, Y. Wang, K. Yang, T.-H. Wei, Y. Song, Solvent effect induced solute damage in an organic inner salt. Opt. Express **18**, 27387–27403 (2010)
25. K. Wang, J. Zhou, L. Yuan, Y. Tao, J. Chen, P. Lu, Z.L. Wang, Anisotropic third-order optical nonlinearity of a single ZnO micro/nanowire. Nano Lett. **12**(2), 833–838 (2012)
26. N. Vamsi Krishna, V.K. Singh, D. Swain, S. Venugopal Rao, L. Giribabu, Optical, electrochemical, third-order nonlinear optical, and excited state dynamics studies of bis (3,5-trifluoromethyl) phenyl-zinc phthalocyanine. RSC Adv. **5**, 20810–20817 (2015)
27. M. Sarma, T. Chatterjee, R. Bodapati, K. Naga Krishnakanth, S. Hamad, S. Venugopal Rao, S.K. Das, Cyclometalated iridium(III) complexes containing 4,4′-π-conjugated-2,2′-bipyridine derivatives as the ancillary ligands: synthesis, photophysics and computational studies. Inorg. Chem. **55**(7), 3530–3540 (2016)
28. J.B. Khurgin, G. Sun, W.T. Chen, W.-Y. Tsai, D.P. Tsai, Ultrafast thermal nonlinearity. Sci. Rep. **5**, 17899 (2015)
29. C. Babeela, T.C. Sabari Girisun, Low temperature phase barium borate: a new optical limiting in continuous wave and nano pulsed regime. Opt. Mater. **49**, 190–195 (2015)
30. S.-K. Min, C.-H. Oh, G.J. Lee, Y.P. Lee, Nonlinear optical properties of ZnO nanorods prepared by using the electro-deposition method. J. Korean Phys. Soc. **55**, 1005–1008 (2009)
31. J. He, W. Ji, G.H. Ma, S.H. Tang, E.S.W. Kong, S.Y. Chow, X.H. Zhang, Z.L. Hua, J.L. Shi, Ultrafast and large third-order nonlinear optical properties of CdS nanocrystals in polymeric film. J. Phys. Chem. B **109**, 4373–4376 (2005)
32. X.-Q. Yan, X.-L. Zhang, S. Shi, Z.-B. Liu, J.-G. Tian, Third-order nonlinear susceptibility tensor elements of CS_2 at femtosecond time scale. Opt. Express **19**, 5559–5564 (2011)
33. G. Yang, A. Chen, M. Fu, H. Long, P. Lu, Excimer laser deposited CuO and Cu_2O films with third-order optical nonlinearities by femtosecond Z-Scan measurement. Appl. Phys. A **104**, 171–175 (2011)
34. T. Hashimoto, T. Yoko, Third-order nonlinear optical properties of sol-gel derived V_2O_5, Nb_2O_5 and Ta_2O_5 thin films. Appl. Opt. **34**, 2941–2948 (1995)
35. M.R. Parida, C. Vijayan, C.S. Rout, C.S. Suchand Sandeep, R. Philip, P.C. Deshmukh, Room temperature ferromagnetism and optical limiting in V_2O_5 nanoflowers synthesized by novel method. J. Phys. Chem. C **115**, 112–117 (2011)
36. C. Yang, Z.J. Shang, Z. Wang, H. Peng, X.D. Tang, B. Li, Y. Chen, Investigation of nonlinear optical properties in bismuth nanospheres suspensions. J. Opt. **44**, 7–11 (2015)
37. U. Pasha Shaik, P. Ajay Kumar, M. Ghanashyam Krishna, S. Venugopal Rao, Microstructural manipulation of nonlinear optical response of ZnO films grown by thermal evaporation technique. Mater. Res. Express **1**, 046201–046218 (2014)
38. K. Jamshidi-Ghaleh, N. Mansour, Nonlinear absorption and optical limiting in Duran glass induced by 800 nm femtosecond laser pulses. J. Phys. D Appl. Phys. **40**, 366–369 (2007)
39. L. Polavarapu, N. Venkatram, W. Ji, Q.-H. Xu, Optical-limiting properties of Oleylamine-capped gold nanoparticles for both femtosecond and nanosecond laser pulses. ACS Appl. Mater. Interfaces **1**, 2298–2303 (2009)